2022

Low-Carbon District Heating: Performance Modeling of Hybrid Solar, Heat Pump and Thermal Storage Systems for District Thermal Energy in the United States

Jordan Tracy Cox

Gustavo Campos

Paul Armatis

Scott Belding

Travis Lowder

See next page for additional authors

Low-Carbon District Heating: Performance Modeling of Hybrid Solar, Heat Pump, and Thermal Storage Systems for District Thermal Energy in the United States

Jordan T. COX[1]*, Gustavo CAMPOS[1], Paul D. ARMATIS[1], Scott BELDING[1], Travis LOWDER[1], Lasse KRISTENSEN[2], Andreas ZOURELLIS[2], Frédéric BLESS[3], Cordin ARPAGAUS[3], Samuel F. BALDWIN[4]

[1]National Renewable Energy Laboratory
Golden, CO, USA
jordan.cox@nrel.gov, gustavo.campos@nrel.gov, paul.armatis@nrel.gov, scott.belding@nrel.gov, travis.lowder@nrel.gov

[2]Aalborg CSP A/S
Aalborg, Denmark
info@aalborgcsp.com

[3]OST-Eastern Switzerland University of Applied Sciences, Institute for Energy Systems
Buchs, Switzerland
frederic.bless@ost.ch, cordin.arpagaus@ost.ch

[4]U.S. Department of Energy (DOE)
Washington, DC, USA
sam.baldwin@ee.doe.gov

* Corresponding author

ABSTRACT

District heating requires thermal energy temperatures ranging from 40°C to 120°C. Typically, the thermal energy input for these systems has been largely met through fossil energy; however, the temperature range is low enough that it presents an opportunity for low-carbon technologies, such as solar thermal and electrified thermal generators like heat pumps (HPs), to decarbonize district heat generation. In this paper, an HP model is applied to estimate the performance and economics of a real-world, low-carbon district heating substation. This system comprises a flat plate solar collector field paired with a mechanical vapor compression HP and hot water thermal storage, augmented by gas-fired boilers. Plant data from a district heating substation in Denmark, provided by Aalborg CSP, are used to tune the model and to estimate the system's benefits in terms of both standard financial metrics (internal rate of return and payback) and environmental metrics, including avoided CO_2 emissions. The model is subsequently employed to estimate the technical and economic potential of solar+HP+thermal storage hybrid systems as retrofits for district heating systems in eight U.S. markets.

1. INTRODUCTION

District heating systems have been in use for centuries but arose in their modern form around the late 1800s (Wiltshire, 2016). District heating systems provide three main advantages over building-level heating systems. First, they can leverage economies of scale to more economically produce thermal energy on a per-kilowatt-hour level. Second, district heating systems can use a combination of energy sources, such as solar, geothermal, or combined heat and power, whereas most building heating systems use one heat source. Third, as countries pursue various decarbonization strategies, district heating systems, as a single large provider of thermal energy, can be a faster route to decarbonization than encouraging individual consumers to change their behavior. District heating systems have been divided into four

or five "generations," with each generation achieving successively lower temperatures, down to 40°C[1] (Buffa et al., 2019). Although district heating systems can be more cost-effective, they are not necessarily more energy efficient because some thermal energy is lost in the network of piping used to transfer the thermal energy, hence the push toward lower district heating network temperatures, which reduce heat losses (Lund et al., 2014).

In addition to these advantages, district heating systems have been considered an important part of decarbonization because of their ability to compensate for variable renewable energy sources using thermal energy storage (TES). A district heating system employing renewable energy, either for direct generation such as geothermal or indirectly through electrically driven heat pumps (HPs), could respond to grid electricity supply (IEA, 2022; Mathiesen et al., 2015). For example, centralized and electrically driven district heating systems with TES could provide demand response at times when variable renewable energy supply is low. Additionally, district heating systems require relatively low temperatures (40°C to 120°C), which makes them a good "first mover" for renewable thermal applications. Currently, 90% of district heating systems globally rely on fossil fuels, making them a prime candidate for decarbonization technologies like HPs (David et al., 2017).

1.1 Heat Pump- and Solar-Assisted District Heating

Electrically driven HPs are heating systems that are very efficient and are commonly used for space heating. HPs act as an energy-efficiency measure because they consume less electricity than the thermal energy they produce. This is because of their ability to "move" heat and use either atmospheric temperatures or waste heat sources to "upgrade" heat to a higher temperature (Moser & Schnitzer, 1985). The ratio by which they convert electricity to usable thermal energy is their coefficient of performance (COP), which is inversely related to the temperature lift that the HP must increase the working fluid.

To compensate for seasonal low atmospheric air temperatures experienced in some regions while maintaining high HP performance, alternative heat sources—such as large or flowing bodies of water or wastewater—that are closer to room temperature than ambient air have been used (David et al., 2017). Standard ambient water temperatures can range from 1°C to 5°C during winter operation, whereas wastewater can range from 15°C to 20°C, although the latter presents a larger capital cost for interconnection and requires colocation with the water treatment facility. Additionally, hybrid district heating systems that use HPs plus solar thermal collectors (referred to in this paper as solar flat plate collectors, FPCs) and TES have also been implemented (Chen et al., 2021; Geyer et al., 2019)

In European countries and in the United States, from where the prices were taken for this study, district heating deployment is estimated at 3.08 GW, which includes hot water (40°C to 100°C) systems and steam systems (>110°C) (Akar et al., 2020; Nielsen & Sørensen, 2016). Solar hot water heaters exceeded 400-GW_{th} capacity in 2017 and continue to increase in use for industrial, building, and district heating applications (Correa-Jullian et al., 2020). As the global capacity has increased, cost declines in both technologies have led to increased adoption for thermal applications, with the effect of reducing emissions due to thermal energy; however, U.S.-based adoption has lagged other countries as a result of the low price of thermal energy from fossil resources, lack of manufacturers, and no nationally directed policy toward carbon reductions (Cox et al., 2022).

1.2 Paper Contributions

The objective of this paper is to estimate the economic competitiveness of a district heating system using an HP under different pricing regimes. To do this, an HP model previously developed at the National Renewable Energy Laboratory (NREL) under public funding from the U.S. Department of Energy (Cox et al., 2022) was used to assess the performance of a real HP-assisted district heating system. Aalborg CSP is a company in Denmark providing renewable and thermal energy engineered systems. In partnership with Aalborg CSP and the Eastern Switzerland University of Applied Sciences (Institute for Energy Systems), NREL implemented the previously developed HP model using data supplied by Aalborg CSP for a real-world district heating substation located in Ørum, Denmark (Aalborg CSP, 2022). The plant comprises a flat plate solar collector field paired with a mechanical vapor compression HP and a TES tank, augmented by gas boilers that supply combined heat and power. A diagram of the plant is shown in Figure 2 in the methodology section of this paper. Weather and operating parameters from the district heating substation were used as inputs for the HP model, the performance of which was compared and calibrated to the measured data from the

[1]Fifth-generation heating systems can be as low as 20°C but are excluded here because they use a distributed rather than a centralized approach to building thermal generation.

Ørum substation. The results of this model were then applied to U.S. regions to estimate HP competitiveness in various price regimes, along with other sensitivities performed.

2. MODELING METHODOLOGY

A model was constructed to estimate the thermodynamic performance of the HP and to evaluate the economics using common profitability metrics. The following sections detail the HP thermodynamic and economic analysis. Finally, the case study inputs are presented along with their associated assumptions.

2.1 Thermodynamic Model

The HP model used for this work has the capability to evaluate HP performance using two methodologies—a Carnot efficiency factor (Chen et al., 2021; Oluleye et al., 2017) and a refrigerant-based approach (Kosmadakis et al., 2020; Wang et al., 2010)—that have been used and are detailed in previous published studies. These two methodologies predict the COP of an HP, which will directly affect HP economics. For this work, the refrigerant of the Ørum substation was known (ammonia, NH_3, R717), and a better understanding of the potential refrigerants for HPs in industrial applications was desired, hence the refrigerant model was chosen.

Figure 1 shows the basic layout of a two-stage mechanical vapor compression HP. The HP cycle configuration was chosen based on the real HP from the Ørum substation, which is described in more detail in Section 2.3. Equations (1) to (6) describe the variable nomenclature used in this work. To model the evaporator and condenser, a 5°C temperature difference is assumed between the refrigerant temperatures and the heat source inlet ($T_{Available}$) and sink outlet ($T_{Desired}$) temperatures, as shown in Equation (1). The heat absorbed in the evaporator, $\dot{Q}_L$, and the heat leaving the condenser, $\dot{Q}_H$, are provided in Equation (2). From the high and low temperatures, the compressor pressure can be estimated to maintain the appropriate phase for the refrigerant, here chosen as ammonia. The real compressor work for each stage can be determined using the compressor isentropic efficiency, ε, and the refrigerant enthalpy, h, at the different steps in the compression process, as shown in equations (3) and (4). As shown later, the compressor isentropic efficiencies were estimated from plant data. The COP, given in Equation (6), can then be calculated as the ratio between the HP thermal output, $\dot{Q}_H$, and the combined compressor work ($W_{C1} + W_{C2}$). Refrigerant flow rates can be determined using equations (2) and (5), the latter showing the flow ratio, r, between the evaporator and the condenser from a mass balance around the flash tank. The HP model calculates the COP on an hourly basis from the desired high temperature, T_H, and the available low temperature, T_L, whereas the HP capacity and the refrigerant flow rate are estimated from the required thermal demand profile, $\dot{Q}_H$ (kWh), and the COP. Currently, the HP model does not adjust compressor efficiency based on transient effects, but it can accept either a constant or varying compressor efficiency (e.g., as a function of pressure ratio or temperature lift).

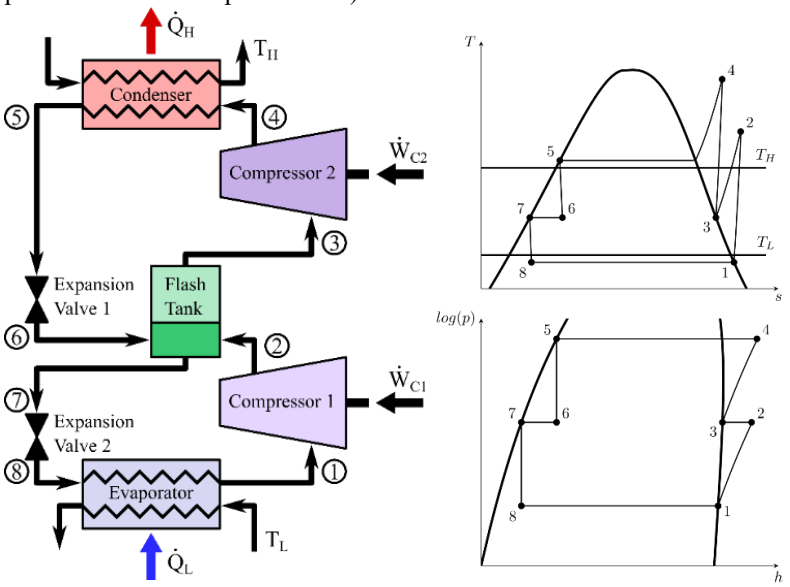

Figure 1: Two-stage vapor compression HP schematic (left) and T-s and p-h diagrams (right) (Figures created by NREL)

$$T_H = T_{Desired} + 5°C, \qquad T_L = T_{Available} - 5°C \tag{1}$$

$$\dot{Q}_H = \dot{m}_H(h_4 - h_5), \qquad \dot{Q}_L = \dot{m}_L(h_1 - h_8) \tag{2}$$

$$\dot{W}_{C1} = \dot{m}_L \frac{(h_2 - h_1)}{\varepsilon_1}\ , \qquad \dot{W}_{C2} = \dot{m}_H \frac{(h_4 - h_3)}{\varepsilon_2} \tag{3}$$

$$\varepsilon_1 = \frac{h_{2s} - h_1}{h_2 - h_1}, \qquad \varepsilon_2 = \frac{h_{4s} - h_3}{h_4 - h_3} \tag{4}$$

$$r = \frac{h_6 - h_3}{h_7 - h_2} = \frac{\dot{m}_L}{\dot{m}_H} \tag{5}$$

$$COP_{Real} = \frac{\dot{Q}_H}{\dot{W}_{C1} + \dot{W}_{C2}} \tag{6}$$

2.2 Economic Model

The economic model is based on a cash-flow analysis where the lifetime levelized cost of heat (LCOH) is calculated by dividing the lifetime HP costs by the lifetime energy produced. For this, one year of energy production is estimated and multiplied by the number of expected years for the HP lifetime (N). The lifetime energy costs are a summation of the HP capital costs (C_O^{HP}) and the annual costs of the ith year (which include energy, fixed operation-and-maintenance (O&M), and variable O&M costs) divided by a discount rate (d). The annual HP costs include fixed O&M estimates based on the capacity thermal energy supplied (\$/kW$_{th}$), variable O&M estimates based on the thermal energy supplied (\$kWh), annual electricity costs per unit (\$/kWh), and demand charges based on the largest monthly electricity demand of the HP (\$/kW). The economic model compares the HP costs to a similarly sized gas boiler with the same calculation for lifetime costs and LCOH but using a boiler efficiency (0.8) in lieu of the HP COP. Full details of the economic calculation are provided in previous literature on the model validation (Cox et al., 2022).

$$Lifetime\ Costs = C_0^{HP} + \sum_{i=1}^{N} \frac{C_i^{HP}}{(1+d)^i} \tag{7}$$

2.3 Case Study: Ørum District Heating System Description

The system considered is a substation of Ørum Varmeværk, a district heating plant in Ørum, Denmark, located approximately 1 mile from the main plant. The substation comprises a solar thermal FPC field, an industrial HP, and a TES tank (Aalborg CSP, 2022), as depicted in Figure 2. The HP has a capacity of 2.5 MW$_{th}$, with an estimated average annual energy production of 10,000 MWh$_{th}$, whereas the FPC field contributes an additional 2,800 MWh$_{th}$. Emissions savings have been estimated at 1,580 metric tons of CO_2 per year. The HP is a custom-made model by Sabroe (similar to the commercial model Sabroe DualPAC) and features ammonia (R717) as the refrigerant and a two-stage compression cycle with open flash inter-cooler. Screw (SAB233SR, 410 kW) and reciprocating/piston (HPC112SV, 389 kW) compressors are used in the low- and high-pressure sides, respectively. The HP operates in parallel to the solar FPC field and can operate both as air-to-water using ambient air as the source or air+water-to-water using both ambient air and intermediate water streams from the TES tank to upgrade its heat content. The air+water-to-water mode is preferred when the solar field is in operation. The substation provides hot water with a supply temperature of approximately 50°C to 65°C, with an annual average COP of 3.7 for the HP. The hot water stream returning to the substation can be sent to either the HP, TES tank, or FPC field. An additional heat exchanger (HXR) is employed to increase the solar thermal efficiency. The TES tank is a single-tank thermocline system.

Aalborg CSP provided hourly data summarizing the total thermal energy supplied by the substation. These data were broken out into the thermal energy provided by the FPC, HP, and the buffer of the TES, as shown in Figure 3. Although data were provided for the full year, one week is shown for legibility. The TES thermal energy supplied can be either positive for discharging or negative for charging.

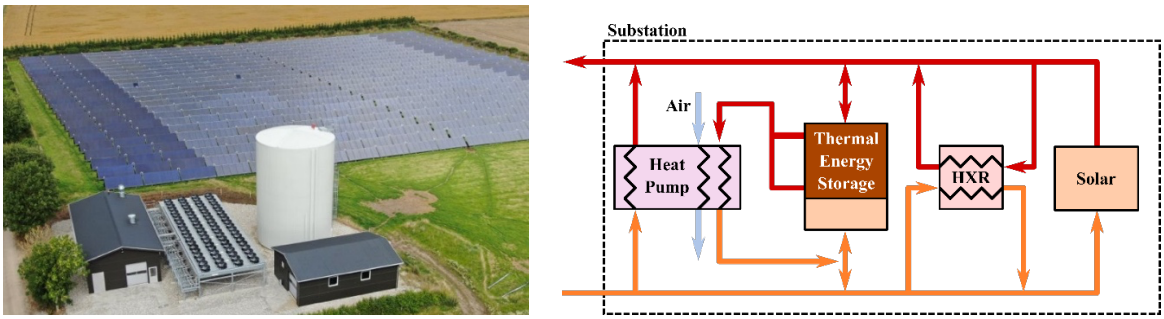

Figure 2: Ørum substation (left) and process flow diagram (right). Photo courtesy of Aalborg CSP

Figure 3: One week of total thermal supply, HP, solar, and TES outputs

Table 1: Fixed financial inputs for the HP economics base case

Parameter	**Value**
Conversion rate (USD/DKK)	0.16 (Bloomberg, 2022)
HP specific capital cost	\$2,000/kW$_e$
HP specific fixed O&M	2% of specific capital cost
HP variable O&M	\$17/MWh
Price of carbon	\$35/metric ton
Discount rate	3%
Denmark average gas rate (2021)	\$102/MWh
U.S. average gas rate (2021)	\$19/MWh
Project lifetime	25 years

The NREL HP model performance was compared to the performance reported by Aalborg CSP to estimate the overall error of the NREL HP model. The summary of inputs for the 'base case' financial model are provided in Table 1. Then, the HP model was applied to the nine economic scenarios, including Denmark electricity and gas prices from 2018–2021, and wholesale electricity prices at eight regional hubs across the United States, with Henry Hub gas prices

used as the standard gas price. The electricity prices from Denmark and the United States are meant to represent real-world cases as best as possible; however, there will be significant uncertainty in variables such as HP capital cost, discount rates, gas costs, and carbon emissions costs. To address these, uncertainty sensitivity scenarios were run. The average annual electricity prices from each location are provided in Table 2 and the hourly electricity prices are graphed for Denmark in Figure 4 and the United States hubs in Figure 5.

Table 2: Electricity and gas prices for HP and boiler inputs (Nord Pool, 2022)

Case	Source	Average Annual Electricity Cost ($/MWh)
Denmark 2018	Nord Pool: Denmark 2018	52.5
Denmark 2019	Nord Pool: Denmark 2019	46.0
Denmark 2020	Nord Pool: Denmark 2020	29.7
Denmark 2021	Nord Pool: Denmark 2021	104.8
U.S. Midwest	EIA: Indiana Hub RT Peak	51.1
U.S. Northwest	EIA: Mid C Peak	59.6
U.S. Texas	EIA: Nepool	53.2
U.S. California North	EIA: NP15	61.5
U.S. California South	EIA: SP15	56.1
U.S. Northeast	EIA: PJM	46.1
U.S. West	EIA: Palo Verde	59.3

Four sensitivity cases were run, with two cases designed to understand the HP economics and two cases designed to understand the gas economic impacts on the HP economics. The cases adjust the HP capital cost, financing costs, gas prices, and carbon prices. The capital cost cases span significant from cost reductions ($1,000/kWe) to high-cost, bespoke HP facilities ($3,500/kWe). The financing costs are estimated by using a discount rate representative of a well-established low-risk technology (2%) to a higher discount rate representing higher financing costs associated with first-of-a-kind projects (15%). The gas sensitivities focus on gas prices ranging from $17/MWh to $150/MWh and carbon costs ranging from $0/metric ton to $200/metric ton (Batini et al., 2020; *Energy Policies of IEA Countries - Denmark 2017 Review*, 2017).

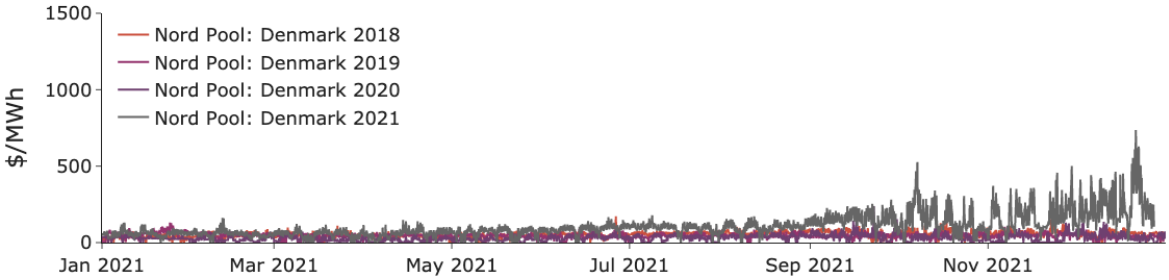

Figure 4: Denmark hub wholesale electricity prices (2018–2021) (Nord Pool, 2022).

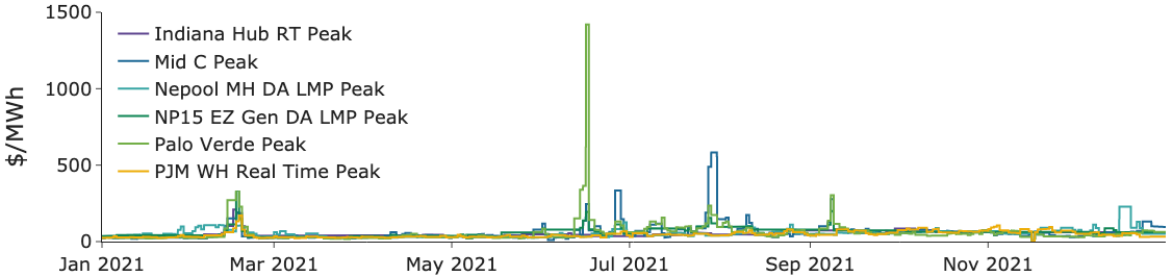

Figure 5: U.S. hub wholesale electricity prices (U.S. Energy Information Administration, 2022).

3. RESULTS AND DISCUSSION

3.1 Heat Pump Performance

Presented first is the comparison between the model-predicted HP performance and the real-world HP data from the Ørum substation. The analyzed data include the hot water flow rate and temperatures at the inlet and outlet of the HP as well as the power consumption of the compressor. Operating and ambient temperatures were taken from the year 2021. The former variables are used to calculate the heat rejected by the HP cycle for water heating, whereas the latter is used to calculate the COP of the HP. As stated previously, the HP can be operated in two ways: air-to-water and air+water-to-water. In the latter, the HP employs both ambient air and intermediate warm water streams from the TES as heat sources. The data set is separated according to the HP mode (i.e., heat source employed).

The compressor isentropic efficiency is known to vary, typically between 50% and 80%, depending on compressor type, application, refrigerant, and operating conditions (e.g., pressure ratio) (ASHRAE, 2016). Although typical values for isentropic efficiency for small-scale, high-temperature HPs have been observed within 50% to 70% (e.g., using data from (Arpagaus & Bertsch, 2019) and (Huang et al., 2017)), higher efficiencies can be expected for high-capacity commercial equipment. The compressor isentropic efficiency was thus estimated by performing a regression (via local optimization) with the air-to-water data as observed at the Ørum plant and was found to be approximately 75% for both low- and high-pressure compressors. The main results of the comparison are presented in Figure 6. The graph on the left presents the COP prediction versus data (the red dashed line represents perfect prediction), which also indicates the range of available data (~2.5 COP to ~4.5 COP). The graph on the right presents the measured and predicted values throughout several operating hours in a year (not necessarily consecutive hours because the HP was not in operation all year). Overall, a good fit was observed, with a mean absolute error of 0.13 COP (3.9% difference relative to the measured COP), and with a standard deviation of 0.09 COP (2.8% deviation with respect to the measured COP). An average COP of 3.32 was obtained for the HP operating in air-to-water mode.

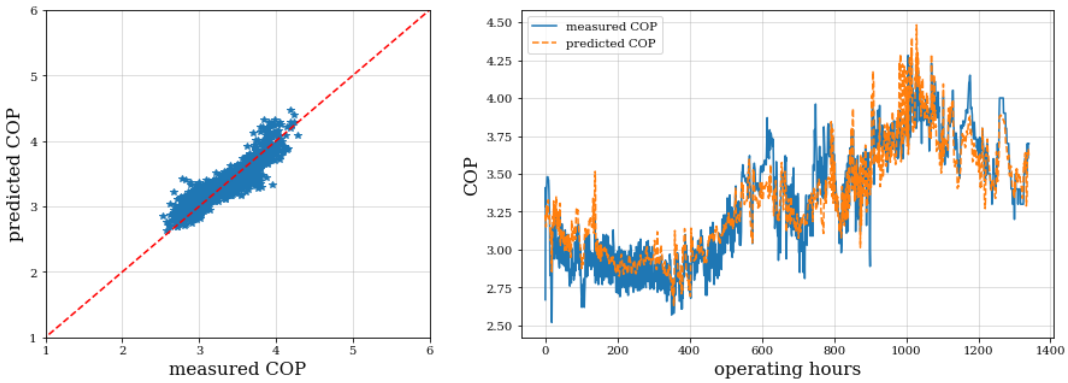

Figure 6: Comparison of HP model-predicted COP with plant data.

Next, the air+water-to-water mode was used to further validate the HP model performance. The compressor isentropic efficiency was fixed at the value obtained in the previous analysis. In this case, the individual effect of air and water on the source temperature is unknown because air flow rate is not measured. A weighted average was assumed for the source temperature, where the weights represent the effect of each source stream (air and water) in the effective source stream temperature. The weights were tuned with a local optimizer and resulted in 10% for water and 90% for air ($T_L = 0.9\,T_{air} + 0.1\,T_{water}$). The comparison of the model prediction with the COP data for the air+water-to-water mode presented similarly satisfactory results, with a mean absolute error of 0.13 COP (3.97% relative to the measured COP) and a standard deviation of 0.14 COP (3.98% relative to the measured COP). An average COP of 3.48 was observed for the air+water-to-water mode, or 3.40 for the combined data set including both air-to-water and air+water-to-water modes.

3.2 Economic and Environmental Performance: Denmark and U.S. Electricity and Gas Prices

The economic results can be separated into three main categories: the Ørum substation in Denmark, the Ørum substation simulated in the United States, and sensitivity analyses. Across all cases, the HP COP performance is the same,

and the HP resulted in an annual emissions savings of 360 metric tons. To reduce the uncertainty of the HP performance, the solar FPC performance was held constant, though this would, of course, change with local solar irradiance and meteorological conditions.

Table 3 shows the results for the Denmark specific cases. For all years examined, the HP demonstrates a strong economic performance. There is a significant sensitivity for the overall HP costs based on electricity prices, which makes the analysis complicated because Denmark electricity prices have significantly shifted during the last four years, and therefore all four years are presented here; however, in all cases, caused by the high cost of gas and the carbon cost, an HP-driven district heating solution makes strong financial sense, with a high net present value (NPV), internal rate of return (IRR), and attractive payback period (PBP).

Table 3: Denmark-based cases (darkest colors: worst economic case, lightest colors: best economic case)

Case	HP LCOH ($/MWh)	Gas LCOH ($/MWh)	NPV ($)	IRR (%)	PBP (Years)
Nord Pool: Denmark 2018	74.8	111.00	222,000	3.9	21.9
Nord Pool: Denmark 2019	74.6		226,000	3.9	21.8
Nord Pool: Denmark 2020	74.0		240,000	3.9	21.7
Nord Pool: Denmark 2021	76.2		186,000	3.7	22.3

In the U.S. price market, we see a much less competitive HP system (Table 4). Although the average electricity prices are similar, it appears that the Ørum substation operated at low electricity prices, and in the United States, for the same operating hours, a much higher LCOH was realized. This suggests both that electricity prices are not a problem for HP performance because they can be operated daily because prices are cheapest when paired with energy storage and that the gas price landscape without a national carbon policy or price continues to be the main barrier to HP adoption in the United States. The U.S.-based gas price without a carbon tax creates a negative NPV for all case tests, meaning that the IRR and PBP are irrelevant. Based on natural gas prices, the two U.S. regions with the most economic competitiveness outside of California were the U.S. northeast and the Southwest. Future work might want to further examine the geographic distribution of U.S. gas prices, though some variables affecting industrial gas prices in the United States might not be relevant for a district heating utility justifying a national average simplification.

Table 4: U.S.-based cases (darkest colors: worst economic case, lightest colors: best economic case)

Case	HP LCOH ($/MWh)	Gas LCOH ($/MWh)	NPV ($)	IRR (%)	PBP (Years)
Indiana Hub RT Peak	90.2	19.0	-2,477,000	N/A	N/A
Mid C Peak	89.0		-2,445,000	N/A	N/A
NP15 EZ Gen DA LMP Peak	90.4		-2,481,000	N/A	N/A
Nepool MH DA LMP Peak	91.9		-2,519,000	N/A	N/A
PJM WH Real Time Peak	88.0		-2,420,000	N/A	N/A
Palo Verde Peak	88.0		-2,422,000	N/A	N/A
SP15 EZ Gen DA LMP Peak	90.3		-2,477,000	N/A	N/A

Finally, the results from the sensitivity studies are shown in Table 5. From the sensitivity cases, the result that has the highest NPV is the case with the lowest HP capital cost. The worst case among the sensitivities run is the result of low gas prices and no carbon cost.

Table 5: Sensitivity cases (darkest colors: worst economic case, lightest colors: best economic case)

Case	Parameter Changed	Case Parameter Value	NPV ($)	IRR (%)	PBP (Years)
Lowest Gas Cost	Gas cost ($/MWh)	17.05 ($5.00/MMBTU)	-1,912,000	N/A	N/A
Highest Gas Cost		136.5 ($40.00 MMBTU)	1,076,000	6.8	14.8
Lowest Carbon Cost	Carbon cost ($/metric ton)	0	2,300	3.0	25.0
Highest Carbon Cost		200	1,258,000	7.4	13.9
Lowest HP Capital Cost	Capital cost ($/kWe)	1,000	1,364,000	11.8	9.2
Highest HP Capital Cost		3,500	-1,492,000	N/A	N/A
Lowest Discount Rate	Discount rate (%)	2	526,000	3.9	19.3
Highest Discount Rate		15	-1,354,000	N/A	N/A

4. DISCUSSION AND CONCLUSIONS

To encourage widescale adoption, HPs need to be both environmentally beneficial and economically competitive. The Ørum substation is a strong example of the potential for good thermodynamic performance and economic competitiveness of HPs for district heating and can help spur more nascent markets to examine HP adoption in several ways. First, the HP performance was predicted within reasonable error (<10%), showing that the NREL-developed HP model can reliably predict HP COP. This is especially useful for cold climates, where HP early adopters are skeptical of HP performance. The Ørum substation is unique in that it uses both ambient air and TES as heat sources to operate the HP at the best efficiencies possible. In the air-to-water mode, the HP showed good COP performance, and by coupling TES and solar, the HP was boosted in a cold climate to provide a consistently competitive COP. It can be concluded that even cold-climate HPs can be integrated into thermal supply with reliable performance bounds. Second, the HP economics were explored for Denmark and U.S. cases as well as for four broad sensitivity scenarios of the combinations of high and low HP costs and high and low gas costs. The United States currently embodies the worst-case scenario, with both high HP costs and low gas prices, whereas Denmark embodies the best case of medium to low HP costs and high gas costs with a carbon cost. Although the Ørum substation HP was not competitive when using the U.S. Energy Information Administration hub electricity prices, the sensitivity analysis shows there are several paths forward for promoting HP competitiveness. For companies that are concerned about future gas prices or voluntarily impose an internal price of carbon, small increases in fossil fuel prices result in a positive NPV for the HP system. Likewise, companies focused on innovation cases where HP capital or financing costs fell also showed positive NPV. Although the cases shown in Table 4 demonstrate that the current U.S. markets are not competitive, the sensitivity results summarized in Table 5 suggest that there are many paths forward for HP competitiveness in the United States or other countries with nascent HP industries.

The work in this paper focuses on predicting HP performance and economics to help build confidence in HPs as a viable thermal energy supply option. Future work should also include pilot cases, industry-developed HP models, robust refrigerant research, and compressor configuration optimization. Additionally, all the cases here assumed that the HP was augmented into an existing district heating system. Novel greenfield developments should also be assessed as new manufacturing operations are examined. HPs represent an important energy-efficiency and clean energy opportunity. From the results, this paper suggests that HPs might be close to adoption, with multiple paths that governments and industries can pursue to further HP competitiveness.

NOMENCLATURE

C	cost	(US$)
COP	coefficient of performance	(–)
d	discount rate	(–)
ε	isentropic efficiency	(–)
h	specific enthalpy	(kJ/kg)
HXR	heat exchanger	(–)
m	mass	(kg)
N	plant life	(yrs)
Q	heat	(kJ)
r	ratio of mass flow rates	(–)
T	temperature	(°C)
W	work	(kJ)

Subscript

e	electric, electricity
H	high temperature
L	low temperature
s	isentropic
th	thermal

REFERENCES

Aalborg CSP. (2022). *Aalborg CSP*. 2.5 MW Integrated Heat Pump System in Ørum, Denmark. https://www.aalborgcsp.com/projects/25mw-integrated-heat-pump-system-in-oerum-denmark/

Akar, S., Kurup, P., MctTigue, J., & Boyd, M. (2020). Renewable thermal hybridization framework for industrial process heat applications. *26th Annual SolarPACES Conference*, 1–8.

Arpagaus, C., & Bertsch, S. S. (2019, September 9). Experimental results of HFO/HCFO refrigerants in a laboratory scale HTHP with up to 150 °C supply temperature. *2nd Conference on High Temperature Heat Pumps*.

ASHRAE. (2016). *HVAC systems and equipment: SI edition*. ASHRAE.

Batini, N., Parry, I., & Wingender, P. (2020). *IMF working paper - Climate mitigation policy in Denmark: A prototype for other countries*.

Bloomberg. (2022, March 24). *USD to DKK exchange rate*. https://www.bloomberg.com/quote/USDDKK:CUR

Buffa, S., Cozzini, M., D'Antoni, M., Baratieri, M., & Fedrizzi, R. (2019). 5th generation district heating and cooling systems: A review of existing cases in Europe. *Renewable and Sustainable Energy Reviews*, *104*, 504–522.

Chen, Y., Hua, H., Wang, J., & Lund, P. D. (2021). Thermodynamic performance analysis and modified thermo-ecological cost optimization of a hybrid district heating system considering energy levels. *Energy*, *224*, 120067.

Correa-Jullian, C., López Droguett, E., & Cardemil, J. M. (2020). Operation scheduling in a solar thermal system: A reinforcement learning-based framework. *Applied Energy*, *268*, 114943.

Cox, J., Belding, S., & Lowder, T. (2022). Application of a novel heat pump model for estimating economic viability and barriers of heat pumps in dairy applications in the United States. *Applied Energy*, *310*, 118499.

David, A., Mathiesen, B. V., Averfalk, H., Werner, S., & Lund, H. (2017). Heat roadmap Europe: Large-scale electric heat pumps in district heating systems. *Energies*, *10*(4), 578.

Energy Policies of IEA Countries - Denmark 2017 Review. (2017). https://www.iea.org/reports/energy-policies-of-iea-countries-denmark-2017-review

Geyer, R., Hangartner, D., Lindahl, M., & Pedersen, S. V. (2019). *Heat pumps in district heating and cooling systems final report annex 47 HPT IEA*.

Huang, M., Liang, X., & Zhuang, R. (2017). Experimental investigate on the performance of high temperature heat pump using scroll compressor. *12th IEA Heat Pump Conference*.

IEA. (2022). *District heating*. https://www.iea.org/reports/district-heating

Kosmadakis, G., Arpagaus, C., Neofytou, P., & Bertsch, S. (2020). Techno-economic analysis of high-temperature heat pumps with low-global warming potential refrigerants for upgrading waste heat up to 150 °C. *Energy Conversion and Management*, *226*, 113488.

Lund, H., Werner, S., Wiltshire, R., Svendsen, S., Thorsen, J. E., Hvelplund, F., & Mathiesen, B. V. (2014). 4th generation district heating (4GDH) integrating smart thermal grids into future sustainable energy systems.

Mathiesen, B. V., Lund, H., Connolly, D., Wenzel, H., Østergaard, P. A., Möller, B., Nielsen, S., Ridjan, I., Karnøe, P., Sperling, K., & Hvelplund, F. K. (2015). Smart energy systems for coherent 100% renewable energy and transport solutions. *Applied Energy*, *145*, 139–154.

Moser, F., & Schnitzer. (1985). *Heat pumps in industry*. Elsevier.

Nielsen, J. E., & Sørensen, P. A. (2016). Renewable district heating and cooling technologies with and without seasonal storage. In G. Stryi-Hipp (Ed.), *Renewable Heating and Cooling* (pp. 197–220). Elsevier.

Nord Pool. (2022). *Nord pool market data*. https://www.nordpoolgroup.com/Market-data1/#/nordic/table

Oluleye, G., Jiang, N., Smith, R., & Jobson, M. (2017). A novel screening framework for waste heat utilization technologies. *Energy*, *125*, 367–381.

US Energy Information Administration. (2022). *Wholesale electricity and natural Gas market data*. https://www.eia.gov/electricity/wholesale/

Wang, K., Cao, F., Wang, S., & Xing, Z. (2010). Investigation of the performance of a high-temperature heat pump using parallel cycles with serial heating on the water side. *International Journal of Refrigeration*, *33*(6), 1142–1151.

Wiltshire, R. (Ed.). (2016). *Advanced district heating and cooling (DHC) systems*. Woodhead Publishing.

ACKNOWLEDGMENTS

This work was authored in part by the National Renewable Energy Laboratory, operated by Alliance for Sustainable Energy, LLC, for the U.S. Department of Energy (DOE) under Contract No. DE-AC36-08GO28308. Funding provided by U.S. Department of Energy Office of Energy Efficiency and Renewable Energy Office of the Principal Deputy Assistant Secretary Strategic Analysis Team and the Advanced Manufacturing Office. The views expressed herein do not necessarily represent the views of the DOE or the U.S. Government. The U.S. Government retains and the publisher, by accepting the article for publication, acknowledges that the U.S. Government retains a nonexclusive, paid up, irrevocable, worldwide license to publish or reproduce the published form of this work, or allow others to do so, for U.S. Government purposes.